

N92-13970

Study of a New Airfoil Used in Reversible Axial Fans

Li Chaojun

Wei Baosuo

Gu Chuangang

Xi'an Jiaotong University
Xi'an, People's Republic of China

Abstract

The characteristics of reversal ventilation of axial flow fan is analysed in the paper. In according to the theory of flow around the airfoil, a new airfoil — "s" shaped airfoil with double circular arc is presented and experimented in the wind tunnel. the experimental results have shown that the characteristics of new airfoil in reversal ventilation is the same as that in normal ventilation and is better than that of existing airfoils of reversible axial fans.

Nomenclature

u	tangential velocity of impeller
c	absolute velocity
w	relative velocity
θ	enter angle of relative velocity of flow
θ_i	installation angle of blade
P_i	theoretical total pressure
$\overline{P_i}$	coefficient of theoretical pressure
ρ	density of flow
r	radius
τ	blade solidity
$\Phi = \frac{c_z}{u_i}$	coefficient of flow rate
c_y	lift coefficient
c_x	drag coefficient
α	attack angle
k	slope of characteristic line of pressure coefficient
b	blade chord
F	half of the maximum thickness of airfoil
\bar{f}	deflection of airfoil ($\bar{f} = \frac{F}{b}$)

Subscript

- 1 before blade cascade
- 2 after blade cascade
- u tangential direction
- z axial direction
- m for mean radius
- o for $\bar{P}_i = 0$
- t tip
- h hub

Introduction

The reversible ventilation of a fan is a problem which often arises in many places, for example, in road and railway tunnels where it is required to drive the air in one or the other direction depending upon the condition that exists at the time. Though an axial fan whose impeller blades are formed with conventional airfoil can drive the air in opposite direction by simply reversing the rotor, it is found that the characteristics of reversal ventilation is much lower than that of the normal ventilation, the efficiency of fan decreasing sharply and the flow rate being about 40-50% of normal ventilation.

The characteristics of reversal ventilation of axial fan with single independent impeller is analysed in the paper. In accordance with the theory of flow around an airfoil, a new airfoil—"s" shaped airfoil with double circular arc is presented. If the impeller blades are formed with such airfoil, the axial fan can operate in each direction to provide a substantially equal but opposite flow with a higher efficiency than can be obtained by existing fan with conventional blades. The reversal ventilation can be achieved by simply reversing the rotor of fan. The "s" shaped airfoil presented in the paper provides a basis for constructing a new type reversible axial fan with simple construction, easy control and better characteristics.

The characteristics of fan impeller during normal and reversal rotation

According to the 2-D cascade theory, the velocity triangle of a blade cascade of the axial fan with single independent impeller is shown in Fig.1.

From the Euler equation

$$P_i = \rho u(c_{2u} - c_{1u}) = \rho u(w_{1u} - w_{2u}) \quad (1)$$

then the coefficient of theoretical pressure is

$$\bar{P}_i = P_i / \rho u_i^2 = u(w_{1u} - w_{2u}) / u_i^2 \quad (2)$$

where u_i is peripheral velocity of impeller.

$$\text{Writting} \quad \bar{r} = \frac{r}{r_i} = \frac{u}{u_i} \quad (3)$$

$$\Phi = \frac{c_z}{u_i} \quad (4)$$

thus the eq.(2) becomes

$$\overline{P_i} = \bar{r}\Phi(tg\theta_1 - tg\theta_2) \quad (5)$$

From fig.1

$$tg\theta_1 = \frac{w_{1u}}{c_z} = \frac{u - c_{1u}}{c_z} = \frac{\bar{r}}{\Phi} - tg\delta_1 \quad (6)$$

According to the cascade theory [4]

$$tg\theta_2 = A tg\theta_1 + B \quad (7)$$

Where

$$A = \frac{1 - \frac{\tau}{4}(dc_y/d\alpha)\cos\beta}{1 + \frac{\tau}{4}(dc_y/d\alpha)\cos\beta} \quad (8)$$

$$B = \frac{\frac{\tau}{2}(dc_y/d\alpha)\sin\beta}{1 + \frac{\tau}{4}(dc_y/d\alpha)\cos\beta} \quad (9)$$

β —the entry angle of relative velocity during $P_i = 0$, i.e. angle of zero lift line (Fig1)

From eq. (5), (6), (7) we get

$$p_i = (1 - A)\bar{r}^2 - \bar{r}\Phi[B + (1 - A)tg\delta_1] \quad (10)$$

The slope of characteristic line of $\overline{P_i}$ is

$$K = \frac{d\overline{P_i}}{d\Phi} = -\bar{r}[B + (1 - A)tg\delta_1] \quad (11)$$

When $\overline{P_i} = 0$, the coefficient of flow rate Φ would have the maximum value

$$\Phi_0 = \frac{(1 - A)\bar{r}}{B + (1 - A)tg\delta_1} \quad (12)$$

and the flow rate becomes maximum too

$$\theta_0 = u_i \int_{r_h}^{r_m} 2\pi r \Phi_0 dr \quad (13)$$

If representing with mean radius r_m

$$\bar{r}_m = \frac{r_m}{r_i}$$

thus

$$\Phi_{om} = (1 - A)\bar{r}_m / [B + (1 - A)tg\delta_1] \quad (12a)$$

$$\theta_{om} = u_i \Phi_{om} \pi(r_i^2 - r_h^2) \quad (13a)$$

It is noted, that the preceding equations are all suitable for both normal and reversal rotating of impeller.

For axial fan with single independent impeller no matter what the rotating direction may be, the air flow into the blade cascade always with axial direction, i.e the angle $\delta_1 = 0$. Making

superscript " ' " for condition of reversal ventilation, thus from the eq. (10), (11), (12a), (13a) the following equations are gotten:

1) the theoretical pressure coefficient

$$\overline{P}_t = (1 - A)\bar{r}^2 - \bar{r}\Phi B \quad (14)$$

$$\overline{P}'_t = (1 - A')\bar{r}'^2 - \bar{r}'\Phi' B' \quad (15)$$

2) the ratio of \bar{K} of reversal ventilation to that of normal ventilation

$$\bar{K} = \frac{K'}{K} = \frac{B'}{B} \quad (16)$$

3) the ratio of maximum theoretical reversal flow rate to maximum theoretical normal flow rate during $\overline{P}_t = 0$

$$J_0 = \frac{\theta'_{om}}{\theta_{om}} = \frac{\Phi'_{om}}{\Phi_{om}} = \frac{(1 - A')B}{(1 - A)B'} \quad (17)$$

Assum that $dc_y/d\alpha$ maintains constant during normal and reversal ventilation, and insert eq.(8), (9) into eq. (16), (17)

$$\bar{K} = \frac{\sin\beta'[1 + \frac{\tau}{4}(dc_y/d\alpha)\cos\beta]}{\sin\beta[1 + \frac{\tau}{4}(dc_y/d\alpha)\cos\beta']} \quad (18)$$

$$J_0 = \frac{ctg\beta'}{ctg\beta} \quad (19)$$

From fig 2

$$\beta = \beta_r - \alpha_0, \beta' = \beta_r + \alpha'_0$$

then inserting into eq.(18).(19)

thus

$$\bar{K} = \frac{\sin(\beta_r + \alpha'_0)[1 + \frac{\tau}{4}(dc_y/d\alpha)\cos(\beta_r - \alpha_0)]}{\sin(\beta_r - \alpha_0)[1 + \frac{\tau}{4}(dc_y/d\alpha)\cos(\beta_r + \alpha'_0)]} \geq 1 \quad (18a)$$

$$J_0 = \frac{ctg(\beta_r + \alpha'_0)}{ctg(\beta_r - \alpha_0)} \leq 1 \quad (19a)$$

From preceding two equations, it is found that J_0 less than 1 and \bar{K} larger than 1 except $\beta' = \beta$ (i.e. $\alpha_0 = -\alpha'_0$). It follows that if the impeller of fan rotates in opposite direction, the maximum flow rate of fan would decrease and the slope of characteristic line of \overline{P}_t would become steep.

Because the α_0, α'_0 are relative with geometrical parameters of blade cascade, such as airfoil deflection \bar{f} , blade solidity τ , installation angle of blade θ , and blade thickness c . therefore J_0 and \bar{K} must be the function of such parameters

$$J_0 = f(\bar{f}, \tau, \theta, c)$$

$$\bar{K} = f(\bar{f}, \tau, \theta, c) \quad (20)$$

From eq. (18a), (19a) if $\beta = \beta'$ (i.e. $\alpha_0 + \alpha'_0 = 0$)

then

$$J_0 = 1, \bar{K} = 1 \quad (21)$$

It means that the characteristics of fan during contrary rotation is the same as that during normal rotation, therefore the best effect of reversal ventilation is obtained.

It is clear that only following two conditions can satisfy the eq.(21)

$$(1) \quad \alpha_0 = \alpha'_0 = 0$$

It can be obtained that if the airfoil deflection $\bar{f} = 0$, such as the flat plate airfoil, ellipse airfoil, the characteristics of such airfoils are lower and not satisfactory for use.

$$(2) \quad \alpha_0 = -\alpha'_0 (\alpha_0 \neq 0, \alpha'_0 \neq 0, \bar{f} \neq 0)$$

It can be obtained when the zero lift line of cascade in reversal ventilation is parallel to that in normal ventilation, i.e. the airfoil must possess the reversal symmetrical profile.

"S" SHAPED AIRFOIL WITH DOUBLE CIRCULAR ARC

On the basis of analysis in preceding section we present a new airfoil—"s" shaped airfoil with double circular arc as shown in fig.3. It is a reversal symmetrical airfoil satisfying the condition $\alpha_0 = -\alpha'_0$. The centre line of the airfoil possesses the shape of "s", which is connected by two circular-arc lines \widehat{ABC} and \widehat{CDE} tangential to each other. At the middle points of two arcs (B,D) the deflection of centre line is maximum.

$$|y_{max}| = F$$

Where F is the half of the maximum thickness of airfoil.

The equations of centre line of airfoil may be written as

$$\begin{aligned} \text{arc } \widehat{ABC} \quad & \left(x - \frac{b}{4}\right)^2 + (y + a)^2 = R^2 \quad x \in (0, \frac{b}{2}) \\ \text{arc } \widehat{CDE} \quad & \left(x - \frac{3b}{4}\right)^2 + (y - a)^2 = R^2 \quad x \in (\frac{b}{2}, b) \end{aligned} \quad (22)$$

$$\text{where } a = (b^2 / 32F) - \frac{F}{2} \quad (23)$$

$$R(\text{radius of circular arc}) = \frac{1}{2} \sqrt{\frac{b^2}{4} + \left(\frac{b^2}{16} - \frac{F}{2}\right)} \quad (24)$$

The formation of airfoil profile

Along the centre line BCD a number of circles with radius $r = F$ are drawn whose centre points are at the arc BCD, then a number of another circles are drawn along the arcs \widehat{AB} and \widehat{DE} , whose centre are at these arcs and whose radii are identified with the perpendiculars from center points to abscissa line x . Drawing envelope line around such circles, the profile of the new airfoil is formed.

If the chord of the airfoil b is constant, taking different value of F , a number of "s" shaped airfoil with different deflection \bar{f} would be obtained.

EXPERIMENTAL RESULT

Four "s" shaped airfoils with different \bar{f} are experimented in wind tunnel in aerodynamic laboratory of Jiaotong University in october 1987. Their symbols are CS-3($\bar{f}=3\%$), C-3.5($\bar{f}=3.5\%$) CS-4($\bar{f}=4\%$) and CS-7($\bar{f}=7\%$).

The experimental results of these airfoils are shown in Fig 4. From fig 4a) It is seen that with the increasing of attack angle α the lift coefficients c_y increase and reach the maximum value then decrease gradually. In the range $\alpha=0^\circ \sim 13^\circ$, the c_y of airfoil CS-4 is the highest among others ($c_{y_{max}}=0.87$) and the c_y of airfoil CS-7 is lower than that of others. From Fig 4 b) it is seen that the drag coefficient c_x of all four airfoils are increased from $\alpha=0^\circ$ and the c_x of airfoil CS-7 is much higher than that of others. In the range of attack angle α from 0° to 10° the c_x of airfoil CS-4 is lower than that of others. It is followed that the aerodynamic characteristic of airfoil CS-4 is better than that of others. Furthermore when the deflection of airfoil is too big ($\bar{f}>7\%$), the drag coefficient c_x of airfoil would increase sharply. The aerodynamic characteristic of airfoil CS-4 is compared with the conventional airfoil (NACA-64, NACA-66). From Fig 5 a), 6 a) it is shown, though the c_y of airfoil CS-4 is lower than that of NACA airfoil in normal ventilation, it is much higher than that in reversal ventilation, especially at bigger attack angle. From Fig 5 b), 6 b) it is seen, in the range $\alpha=0 \sim 10^\circ$ the drag coefficient c_x of airfoil CS-4 is lower than that of NACA airfoil in normal ventilation, while $\alpha > 10^\circ$ it is higher than that of NACA airfoil, but in reversal ventilation condition the c_x of airfoil CS-4 is much lower than that of NACA airfoil in all range of attack angles in experiment.

In order to analyse the flow around the "s" shaped airfoil, the pressure distribution along the surface of airfoil CS-3 at $\alpha=4^\circ$ is measured as shown in Fig 7. There are two areas bounded by pressure coefficient c_p line of airfoil. The area on the preceding half of airfoil ($x/b=0 \sim 0.5$) is positive, which indicates that the lift force on the airfoil is upward; The area on the rear half of airfoil ($x/b=0.5 \sim 1.0$) is negative, which indicates the lift force on the airfoil is downward. Since the preceding area is bigger than the rear area, so the summary lift force on the airfoil is upward. Varying the attack angle α , the two areas and the summary lift force would be changed.

In the Fig 7. $c_p = (P_i - P_0) / \frac{1}{2} \rho c_\infty^2$, where P_i is the pressure at the surface of airfoil. P_0 is the ambient pressure, c_∞ is the flow velocity in the wind tunnel.

Conclusion

1) If the impeller of axial fan with conventional airfoil rotates in reversal direction, the maximum theoretical flow rate would decrease, the characteristic line of P_f become steep, the

characteristics of fan would be worse.

2) The characteristic of impeller in reversal ventilation is identical with that in normal ventilation, when the deflection of airfoil $\bar{f}=0$ or $\bar{f}\neq 0$ but the profile of airfoil is reversal symmetrical.

3) The "s" shaped airfoil presented in the paper is a reversal symmetrical airfoil. When the impeller whose blade is formed with such airfoil rotates in opposite direction, its characteristic would be the same as that in normal ventilation.

4) The synthetical characteristic of axial fan whose impeller blade is formed with "s" shaped airfoil would be better than that formed with conventional airfoil, especially in reversal ventilation condition, therefore the new airfoil presented in the paper is more available for reversible axial fan.

Reference

1. Radha krishna, H.C. Aswa Thanarayana, P.A. and Ramachandran, Rm. "Some Flow Studies on "s" Cambered Aerofoils" Proceeding of Conference on Fluid Machinery, 1979 Budapest.
2. Ravindram, M. and Radha Krishna, H.C. "Influence of Blade Profiles on the Performance of a Fully Reversible Axial Pump-turbine" Proceeding of Conference of Fluid Machinery, 1979 Budapest.
3. Ravindram, M. and Radha Krishna, H. C. "Characteristics of a Fully Reversible Axial Pump-turbine for Application in Tidal Power Plants" Paper presented at the Conference on Future Energy Concept, Orgaized by IEE, London, Jan-Feb 1979.
4. Longhua Li "Feasibility study of inverse ventilation in Chinese coal-mines by simple reversing the axial fan" The 2nd China-Japan Conference on Fluid Machinery, 1989 Xi'an China.

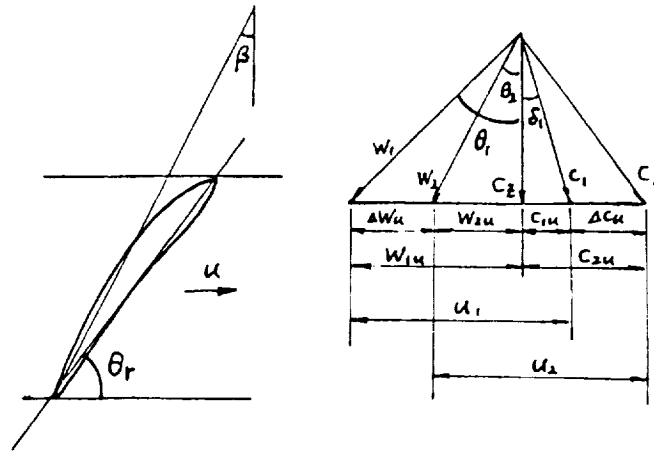


Fig.1. The velocity triangle of a blade cascade

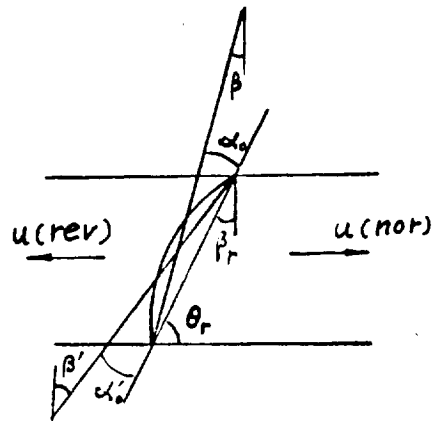


Fig.2. Normal and contrary flow around an airfoil

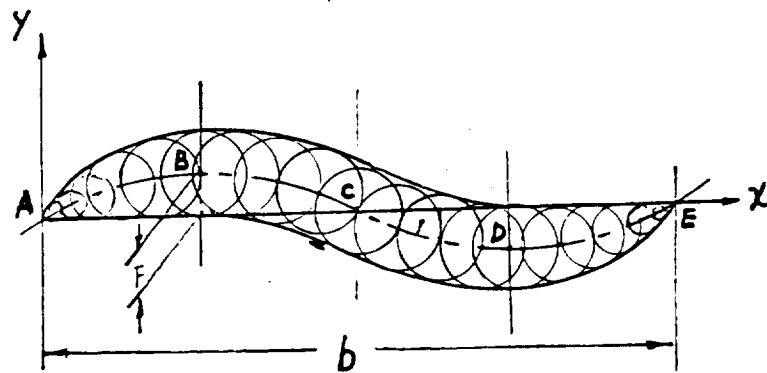


Fig.3. "S" shaped airfoil with double-circular arc

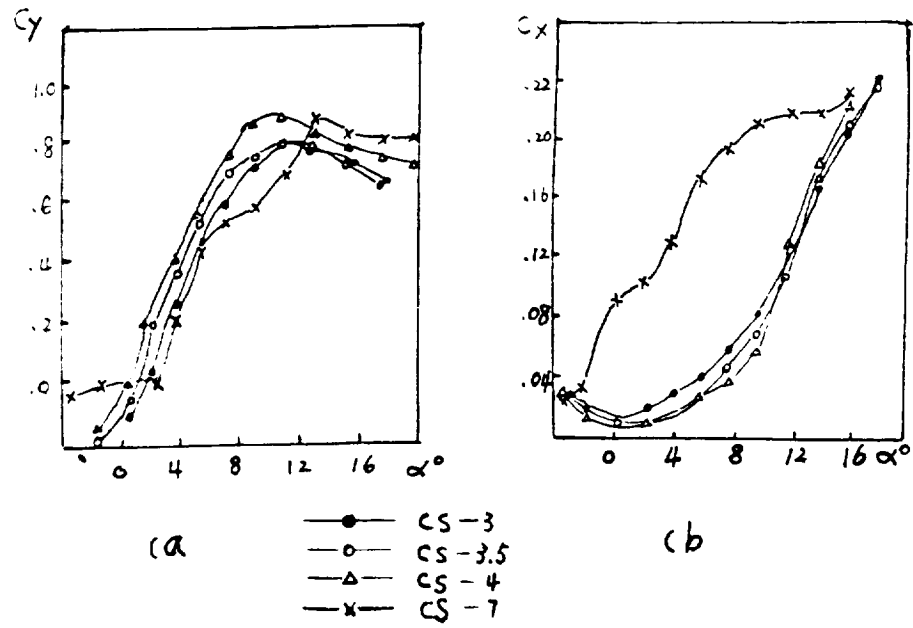


Fig.4. The experimental results of CS-4 airfoil series

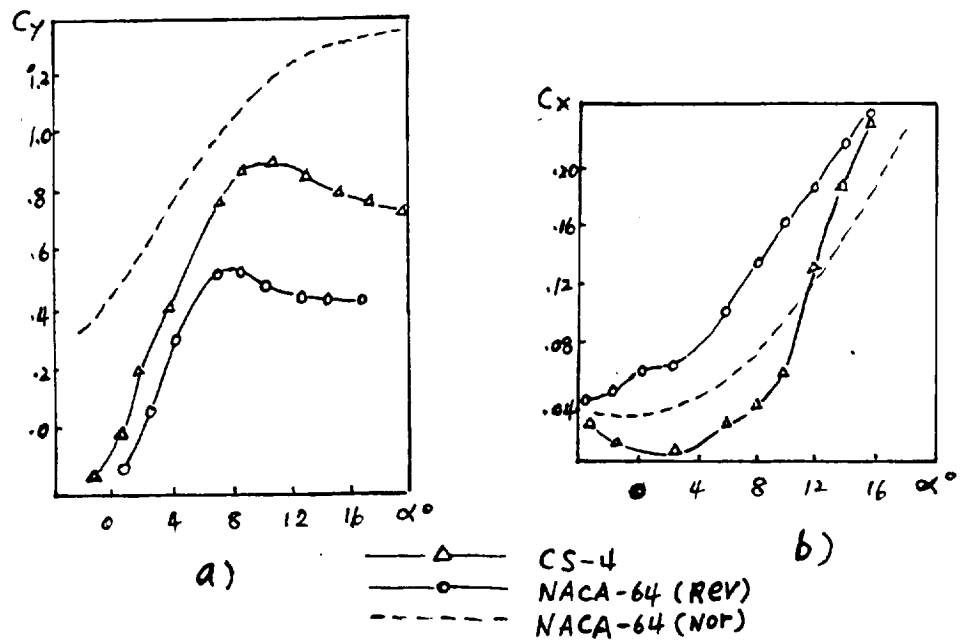


Fig.5. Comparison of airfoil CS-4 with conventional airfoil NACA-64 in normal and reversal ventilation

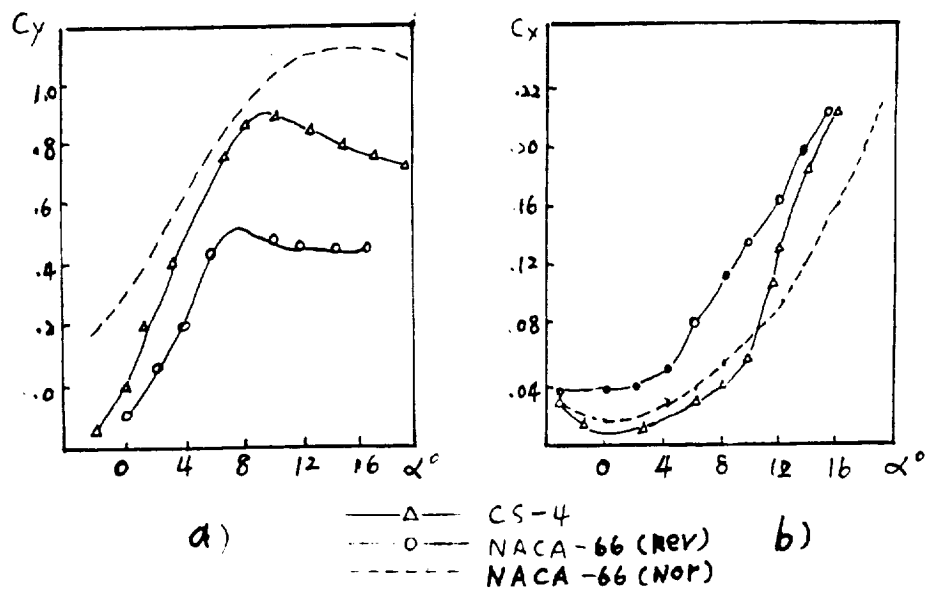


Fig.6. Aerodynamic characteristic comparison of CS-4 airfoil with airfoil NACA-66 in normal and reversal ventilation

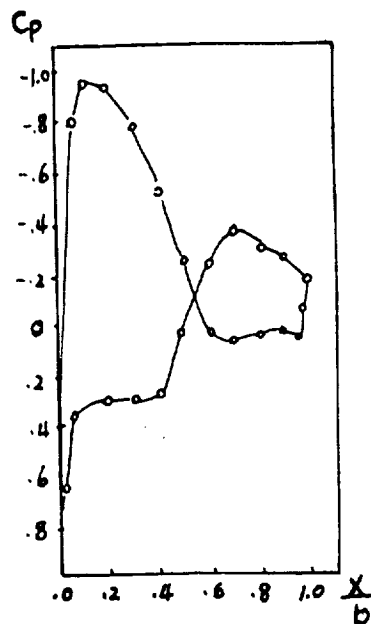


Fig.7. The pressure distribution along the surface of airfoil CS-3.